Available online at www.sciencedirect.com
ScienceDirect
Surface Science 601 (2007) 2473–2485
SURFACE SCIENCE
www.elsevier.com/locate/susc

A DFT study of the chemisorption of methoxy on clean and low oxygen precovered Ru(0001) surfaces

M. Natália D.S. Cordeiro *, Ana S.S. Pinto, José A.N.F. Gomes

REQUIMTE/Departamento de Química, FCUP, Rua do Campo Alegre 687, 4169-007 Porto, Portugal

Received 23 February 2007; accepted for publication 12 April 2007
Available online 4 May 2007

Abstract

Adsorption of the methoxy radical on clean and on low oxygen precovered Ru(0001) metallic surfaces has been studied by density-functional theory cluster calculations. Methoxy is predicted to be preferentially chemisorbed on both hollow sites (hcp and fcc) of such surfaces, and adopts an upright orientation (C_{3v} local symmetry). Such prediction is supported by the good agreement found between the calculated vibrational frequencies and the experimentally observed RAIRS spectra. Regarding the charge transfer process between the adsorbate and the surface, our results suggest that the bonding is dominantly polar covalent which arises from a charge donation from the ruthenium surface to the radical, and the co-adsorbed electronegative oxygens deplete slightly the surface electron density. However, the major difference is not induced through much O–Ru bonding, but indirectly, by lowering the valence d-band center of the system. This results in a lower adsorption energy for methoxy than on the clean Ru(0001) surface, in accordance with experimental data. Further, accordingly to the present calculations, the radical is expected to dissociate or desorb more easily on the modified surface but with no participation from the co-adsorbed oxygen atoms.

Keywords: Density functional calculations; Chemisorption; Radical methoxy; Effect of ad-atoms

1. Introduction

Many commercially important products can be prepared with high efficiency depending upon the use of transition metal surfaces as catalysts [1]. For instance, the catalytic oxidation of methanol is a key industrial process in the development of fuel cells, and such cells display clear benefits over combustion engines and hydrogen-based cells [2–8]. This has lead to an extensive research on the reaction of methanol with clean and modified single-crystal metal surfaces [9–27]. Besides, methanol is a prototype polyatomic organic molecule well suited for surface chemistry studies, since it is relatively simple and yet contains C–H, C–O and O–H bonds. On most surfaces, methanol undergoes O–H bond scission either directly or through reaction with pre-adsorbed oxygen, yielding adsorbed methoxy (CH_3O) [10,14,28]. The methoxy species has been identified on a vast number of metal surfaces, like Ru(0001) [29–34], Ni(100) [35,36], Mo(110) [37], Cu(111) [14,38] or Cu(100) [39–41] to name but a few. However, the experimental determination of the adsorption site of this species with respect to the surface and, especially, the adopted conformation has been far from trivial [37–45]. On the other hand, theoretical calculations have contributed to further the understanding of methoxy adsorption [6,15–27,41–45].

On clean Ru(0001), early work by Hrbek et al. [29], based on energy electron loss spectroscopy (EELS) data, pointed up to an upright orientation for the adsorbed methoxy at low coverage and temperature. Following work by Sasaki et al. [31] suggested instead a non-upright orientation for CH_3O on clean Ru(0001) at low temperature, from electron-stimulated desorption ion angular distribution (ESDIAD) images. More recently, Barros et al. [32] studied the decomposition of methanol on clean Ru(0001) using reflection–absorption infrared spectroscopy (RAIRS). The

* Corresponding author. Tel.: +351 22 6082802; fax: +351 22 6082959.
E-mail address: ncordeir@fc.up.pt (M.N.D.S. Cordeiro).

0039-6028/$ - see front matter © 2007 Elsevier B.V. All rights reserved.
doi:10.1016/j.susc.2007.04.168

authors analyzed the resulting RAIRS spectra taking into account only the fundamental modes. They also concluded that, at low temperature (90 K) and exposure (0.1 L), methoxy is adsorbed with its C–O bond tilted towards the surface plane. However, that conclusion was supported mainly by the observation of a small ρCH_3 band, a mode that is often too weak to be clearly identified in the RAIRS spectra. Further, their assignments of the CH stretch region can be misleading since that region is often perturbed by Fermi resonance between the fundamental stretching mode(s) and overtone CH_3 bending modes [36–45]. Later on, the authors investigated the adsorption of the partially deuterated methanol isotopomer (CHD_2OH) as the CH stretch region of this species is free of Fermi resonance [46]. They recorded the RAIRS spectra upon exposing the clean Ru(0001) surface to an extremely low dose (0.01 L) of CHD_2OH at 90 K. Only one band was detected in the νCH region of CHD_2OH, reinforcing the idea that methoxy adsorbs in an upright orientation at low coverage. Lately, Barros et al. [33,34] analyzed as well the adsorption of methanol on oxygen modified Ru(0001) surfaces. Using RAIRS, they showed that the decomposition of CH_3OH is promoted yielding also adsorbed methoxy at low temperature and exposure. Again, a tilted orientation was proposed for CH_3O but, as the authors argued, that might result from coverage effects even for such a low exposure (0.05 L). This may be indeed the case, judging from their latest RAIRS work on the adsorption of an extremely low dose (0.01 L) of CHD_2OH over the same oxygen modified Ru surfaces [47,48].

In contrast, only a few theoretical studies can be found in the literature concerning the reactivity of methanol on Ru surfaces. Ishikawa et al. [22] studied the adsorption of methanol and other species pertaining to its electro-oxidation, by performing density functional theory (DFT) calculations on a (10-atom) cluster, but reported no results for the adsorbed methoxy. Most recently, we have carried out DFT calculations of CH_3O on clean Ru(0001), which was modeled by a (13-atom) cluster, mainly to provide a better assignment of the C–H stretch region of the observed RAIRS spectrum [49].

The present work reports a detailed study of the adsorption of methoxy on clean and oxygen modified Ru(0001) surfaces *in the low coverage regime*. It complements and extends our preliminary DFT study on the clean Ru(0001) surface [49]. Emphasis is given to the effect of preadsorbed oxygen on the properties of adsorbed methoxy and the results are compared to the experimental data reported by Barros et al. [32–34,46–48].

2. Methods

Both the clean and oxygen modified Ru surface were described in the present work, as in our previous study [49], by cluster surface models. Although periodic slab models of the surfaces would be more realistic, those still require heavily optimized, time-consuming calculations in the limit of low coverages. In addition, such calculations are normally performed within DFT and thus, the calculated results depend on the particular choice of the exchange-correlation functional; in some cases, the uncertainty caused by the choice of a given potential is of the order of that setup by the use of a cluster model [50–56]. Besides the cluster approach remains quite a useful model to predict local properties such as adsorption geometries and vibrational frequencies for extremely low coverages – in fact, the main goal of the present work, provided that some care is taken to evaluate possible cluster-size effects. This is accomplished here by comparing the results obtained from cluster models of different size and shape, i.e., from Ru_n clusters with $n = 13$–28. The specific clusters used for the clean Ru(0001) surface are shown in Fig. 1. The smallest surface cluster model – Ru_{13}, used in our previous study [49], contains two layers of atoms for modeling the coordination at all possible adsorption sites, i.e., hollows (hcp, fcc), bridge and top sites, while the larger clusters, also with two layers of atoms, model only some particular sites to dissect possible cluster-size effects (hcp: Ru_{22}(12,10); fcc: Ru_{18}(12,6); bridge: Ru_{22}(14,8); top: Ru_{22}(10,12); fcc and hcp: Ru_{28}(18,10)). In all cases, the Ru–Ru distances are fixed at the experimental bulk distance ($a_{Ru\sim} = 2.7$ Å) [57].

All electronic structure calculations were performed at the DFT level. These resorted to the B3LYP hybrid functional [58] included in the GAUSSIAN98/03 program [59], which comprises the local correlation functional III of Vosko et al. [60], rather than their recommended functional *V*, together with the non-local correlation functional of Lee et al. [61]. Here, it is important to note that the B3LYP hybrid functional has found wide applicability in molecular calculations; in particular, is able to reproduce the thermochemistry of systems containing transition metal atoms [62–64] as well as describe their chemical reactions with high accuracy [56,65]. The ruthenium atoms were described by the relativist effective (small-)core potential of Hay and Wadt [66–68] that includes the 16 valence electrons explicitly in the calculations. The valence basis sets of double-zeta quality (LANL2DZ) or single-zeta quality (LANL2MB), also reported by Hay and Wadt [66–68], were used for the Ru atoms. The LANL2DZ basis set is used for all Ru atoms of the clusters with $n = 13$–22, while a mixed basis set is adopted for the Ru atoms of the $n = 28$ cluster, namely LANL2DZ (for the three or four atoms defining the hollow sites fcc and hcp, respectively) and LANL2MB (for the remaining atoms). The non-metallic atoms (O, C and H) were described by the all-electron standard 6-31G** basis set. With this B3LYP/LAN/6-31G** approximation, calculations of the density-of-states (DOS) [69] and the crystal orbital overlap population (COOP) [70], which enables the calculation of the overlap of a specific orbital on the adsorbate with the sp and d electronic states of the metal cluster, were carried out for the several systems using program GaussSum [71]. Since the finite nature of the clusters yields discrete energy levels, the

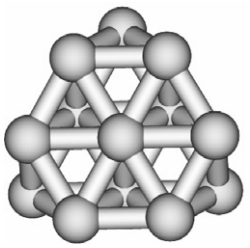

Ru_{13}(7,6): fcc, bridge and top sites; Ru_{13}(6,7): hcp site

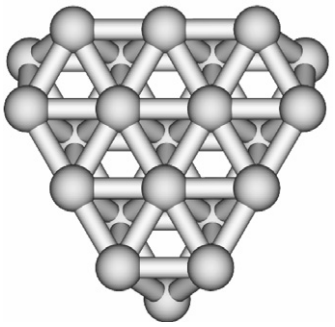

Ru_{22}(12,10): hcp site; Ru_{22}(10,12): top site

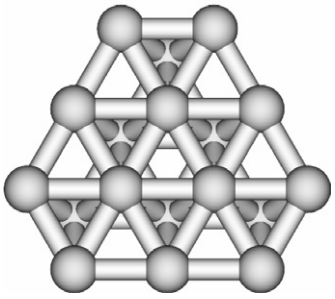

Ru_{18}(12,6): fcc site

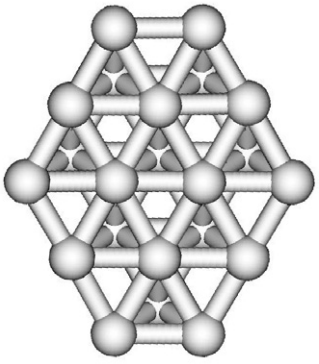

Ru_{22}(14,8): bridge site

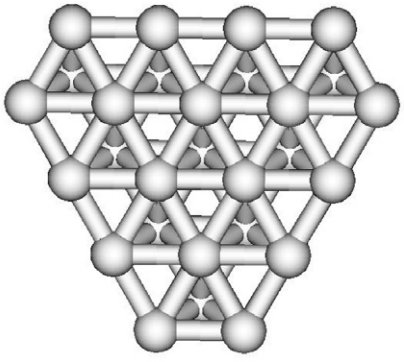

Ru_{28}(18,10): fcc and hcp sites

Fig. 1. Ruthenium clusters used to model the adsorption of methoxy on the clean Ru(0001) surface. The clusters shown are the best models for the particular adsorption site(s) indicated and the figures in parentheses denote the number of atoms in each atomic layer.

electronic states are artificially broadened by a Gaussian of full width at half maximum FWHM (usually, FWHM = 0.3 eV) to simulate an infinite surface.

The free fully-optimized adsorbate has been placed on all possible adsorption sites of the Ru(0001) surface, forcing it to be bound to the surface via the oxygen atom. Then,

partial geometry optimizations were performed in which the metal atoms have been kept frozen in their positions (and also the positions of the preadsorbed oxygen atoms in the case of the Ru(0001)–(2 × 2)–O surface). A word of caution here, an unrelaxed substrate is used in the present calculations, but no strong surface relaxation is to be expected on a hexagonally closed packed surface such as Ru(0001) or even on the modified Ru surface for such a low oxygen pre-coverage (0.25 ML), as judging from published data of low-energy electron diffraction (LEED) intensity analyses [72] as well as DFT-periodic slab calculations [56,72]. Harmonic vibrational frequencies are computed by partial diagonalization of the Hessian matrix [73], and scaled by a factor of 0.9613 as recommended by Scott and Radom [74]. Adsorption energies are calculated as usual, by the difference between the total energy of the cluster–adsorbate super-system and the total energies of the cluster plus the CH_3O isolated fragments. The basis set superposition errors are checked also and found to be within 0.2–0.5 eV, according to the counterpoise technique [75].

Before closing this section, it should be noticed that a hydrogen atom was deliberately incorporated into the clusters, placing it as far as possible from CH_3O, to obtain final singlet closed-shell electronic states for all adsorbate-cluster systems. That enabled us to overcome the severe convergence problems we met when performing open shell calculations on those systems. Nevertheless, it seems reasonable, since the adsorbed methoxy is produced following dissociation of methanol into the CH_3O and H radicals, and a closed-shell electronic structure is the natural choice to model an extended surface. Moreover, Ricart et al. [76] have shown that the choice of the electronic state does not largely affect the basic bonding mechanisms.

3. Results and discussion

3.1. Adsorption of CH_3O on the clean Ru(0001) surface

3.1.1. Structures and energetics

To begin with, one should examine the influence of the surface model on the structural and energetics properties of adsorbed methoxy. Table 1 presents the calculated results for the adsorption of radical methoxy over the different Ru_n clusters modeling the clean Ru(0001) surface.

Let us first consider the data calculated using the smallest Ru_{13} cluster model. As can be seen, methoxy is predicted to be chemisorbed on all possible adsorption sites of the clean Ru surface. It adopts a tilted orientation with respect to the surface on the top and bridge adsorption sites but more upright orientations on the hollow sites. Yet, from these results, most probably affected by edge effects, it is impossible to establish the most favorable site for the adsorbed methoxy. In principle, cluster edge effects can be checked by further increasing the cluster size. Therefore, new calculations were carried out using the larger cluster models referred to in Section 2. Notice that such extended clusters are more free of edge effects, thus likely more realistic, and display higher site symmetry (see Fig. 1). The results in Table 1 clearly show the preference of the adsorbed CH_3O to sit on the hollow sites of the clean Ru surface: the largest binding energy is found for the fcc and hcp sites, followed by the bridge and top sites. They corroborate as well the adopted upright orientation on the hollow sites and the tilted one on top and bridge sites. As before, the tilting on the top site is greater than that of the bridge site and the adsorbate–surface distances on both these sites are higher than those of the hollows, therefore raising the free motion of the methyl group. Similar to many other transition metal surfaces [15–46], the fcc site seems to be the most favorable one for CH_3O adsorption. But the rather small energy difference between the fcc and hcp sites (<0.05 eV) suggests that both will be populated (within the uncertainty of the present calculations) alike to what has been recently found for the Cu(111) surface [26,38].

By comparing the results in Table 1, one can immediately see the inadequacy of the former small cluster model, Ru_{13}, in describing the adsorption properties of the clean surface. For the hcp and bridge sites, the Ru_{13} model may be regarded as essentially converged in view of the rather moderate deviations induced by the cluster-size increase. However, for the top and fcc sites, methoxy on the Ru_{13} cluster is calculated to be much

Table 1
Calculated properties of CH_3O adsorbed on the clean Ru(0001) surface represented by several cluster models

Cluster	Layers	Site	E_{ads} (eV)	d(O-Surf) (Å)	ang(C–O–Surf) (°)	$q_{adsorbate}$ (a.u.)[a]
Ru_{13}	(7,6)	Top	−1.88	2.05	116	−0.23
	(7,6)	Bridge	−1.86	1.75	133	−0.20
	(7,6)	fcc	−1.64	1.76	172	−0.23
	(6,7)	hcp	−2.22	1.58	179	−0.26
Ru_{22}	(10,12)	Top	−1.47	2.06	115	−0.19
Ru_{22}	(14,8)	Bridge	−2.02	1.68	137	−0.19
Ru_{18}	(12,6)	fcc	−2.34	1.50	179	−0.21
Ru_{22}	(12,10)	hcp	−2.31	1.50	179	−0.21
Ru_{28}	(18,10)	fcc	−2.40	1.46	179	−0.25 (**−0.30**; *−0.34*)
	(18,10)	hcp	−2.37	1.42	179	−0.24 (*−0.33*)

[a] Effective charges calculated from Mulliken population analysis save for the ones shown in parenthesis that were computed either from the dipole moment versus surface distance plot (in bold; Fig. 2) or from natural population analysis (in italic).

weaker bound (by ca. 30%) when compared to the larger models, even though with an essentially equal optimized top-structure but rather different fcc-structure (which has a markedly longer surface–O distance). The intermediate Ru_{13} cluster model is thus not large enough to provide reliable converged adsorption properties, particularly for the fcc site; most likely, the smallest model reaching convergence for this site is the Ru_{18} cluster. For a definitive answer, one may take the results obtained using the largest cluster model Ru_{28} as reference. Judging from the attained results (Table 1), convergence with respect to cluster size has, in practical terms, been achieved for the Ru_{18} model (fcc); the same holds for the Ru_{22} model (hcp). Therefore, taking into account the highly demanding computational time needed for the Ru_{28} model, we choose the clusters Ru_{18} (fcc) and Ru_{22} (top, bridge and hcp) to study further features concerning the adsorption of methoxy on the clean surface. Naturally, for reaching particularly accurate (absolute) energy values, larger models or different representations of the surface (e.g., three-dimensional nanoscale cluster models [77]) should be considered.

The interaction of methoxy with Ru(0001) involves electron transfer between the metal substrate and the adsorbed species. The computed Mulliken charges (Table 1) show that the surface donates charge to the adsorbate, and the major part of it comes from the Ru atoms placed near the site where the adsorption occurs. Notice also that the effective charges of the adsorbate follow the trend of the adsorption energies, i.e., the highest charges correspond to the most stable adsorption sites (hollows).

The way in which the total number of electrons of a system can be divided among the contributions of the atomic orbitals is not unique and the Mulliken population analysis is one possibility, though it is known to be highly sensitive to the choice of basis set [78]. However, differences between Mulliken populations before and after adsorption are a reliable tool to investigate charge transfer and, as we will show, good agreement is obtained with other methodologies. Table 1 also lists the effective charge of the adsorbate on the hollow sites calculated with a more refined wave function-based method, i.e., the natural population analysis (NPA), which solves most of the problems of the Mulliken scheme by construction of a more appropriate set of (natural) atomic basis functions [79], and from the slope of the dipole moment curve versus the adsorbate-surface distance (see Fig. 2). As can be seen, there is a good agreement between both methods of estimating the adsorbate effective charge for the fcc adsorption site, since the slope of that curve (−0.30 e) is close to the values obtained by the Mulliken analysis (Ru_{28}: −0.25 e) and NPA (Ru_{28}: −0.34 e), as well as for the hcp site. In addition, the typical linear behavior seen on the dipole moment plot provides an indication of the ionic component of the bonding, excluding polarization effects [80]. Nevertheless, a slope for the dipole moment curve particularly far from 1, like the one obtained here, is characteristic generally of a covalent bond [80]; thus, most likely, the actual character of the methoxy bonding should be polar covalent.

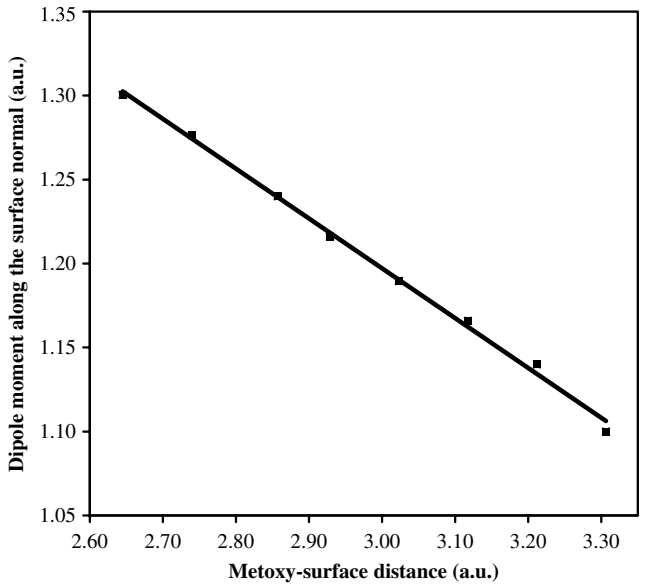

Fig. 2. Variation in dipole moment (1 a.u. = 2.54 D) along the surface normal versus the CH_3O-surface distance for the fcc adsorption site. The slope of the dipole moment curve is −0.30.

3.1.2. IR vibrational spectra

In order to compare the results above directly with the experimental RAIRS data [32,46], vibrational frequency calculations were performed for CH_3O adsorbed on all possible sites of the clean Ru(0001) surface as well as for its isotopomer CHD_2O on the hollows. As the experimental information is limited, only those selected modes for which experimental data is available are reported (Tables 2 and 3). Notice also that the experimental results for CH_3O refer to upper coverages (0.1 L) than those for CHD_2O (0.01 L), the latter affording a more reliable comparison with the present results.

The binding of the methoxy radical to the Ru surface is well characterized by the νCO vibrational mode. The computed values of νCO are shifted to lower wavenumbers for all adsorption sites (especially in the hollows; Table 2) when compared to the corresponding free methoxy (1079 cm^{-1}), suggesting that the oxygen is bonded to the metal. In fact, the C–O bond should be weakened by strong metal–oxygen coordination, with the consequent shift of the νCO mode to lower wavenumbers [32]. Due to this shift, the order of the ρCH_3 and νCO modes inverts when the radical adsorbs on the surface. For the free CH_3O, the $\rho CH_3(A'')$ and $\rho CH_3(A')$ vibrations are located at lower wavenumbers (at 730 and 933 cm^{-1}, respectively) than the νCO vibration (at 1079 cm^{-1}). For the adsorbed methoxy the ρCH_3 modes exceed νCO, regardless of the adsorption site (Table 3). Methoxy adsorption on the surface also results in a red shift of the $\delta_s CH_3$ deformation vibration from 1476 cm^{-1} for free CH_3O to 1325 cm^{-1} (top),

Table 2
Comparison of experimental and calculated vibrational wavenumbers for CH_3O adsorbed on the clean Ru(0001) surface

Mode[a]		Experimental[b]	Calculated			
		(C_s)	Ru_{22}-top (C_1)	Ru_{22}-bridge (C_1)	Ru_{18}-fcc (C_{3v})	Ru_{22}-hcp (C_{3v})
νCO	(A_1/A′/A)	1005	1027	994	1017	1010
ρCH_3	(E/A″/A)	1139	1047	1114	1143	1135
ρCH_3	(E/A′/A)		1089	1125		
$\delta_s CH_3$	(A_1/A′/A)	1435	1325	1386	1407	1407
$\nu_s CH_3$	(A_1/A′/A)	2816	2720	2782	2837	2834
$\nu_{as} CH_3$	(E/A″/A)	2926	2769	2860	2908	2908
$\nu_{as} CH_3$	(E/A′/A)	2949	2863	2899		
MAD[c]			88	36	18	17

[a] Irreducible representations of the modes for $C_{3v}/C_s/C_1$ symmetric species are shown in parenthesis.
[b] RAIRS data obtained upon exposure to 0.1 L of CH_3OH at 90 K [32], save for $\delta_s CH_3$ which was obtained by EELS [29].
[c] Mean absolute deviations with respect to the experimental data.

Table 3
Comparison of experimental and calculated vibrational wavenumbers for CHD_2O adsorbed on the clean Ru(0001) surface (C_s symmetry)

Mode	Experimental[a]	Calculated	
		Ru_{18}-fcc	Ru_{22}-hcp
$w CD_2 + \nu$CO	942	950	947
$w CD_2 + \nu$CO	1012	1017	1011
$\delta_s CD_2$	1071	1052	1051
$\nu_s CD_2$	2111	2068	2068
νCH	2938	2886	2885

[a] RAIRS data obtained upon exposure of 0.01 L of CHD_2OH at 90 K [46].

1386 cm^{-1} (bridge) or 1407 cm^{-1} (fcc and hcp) for adsorbed CH_3O. Likewise, the $\nu_s CH_3$ stretching mode is red-shifted with respect to the corresponding mode computed for the gas-phase radical (=2801 cm^{-1}). As to the antisymmetric stretching mode $\nu_{as} CH_3$, its position depends on the local structure of the adsorption site. The calculated frequency for the gas-phase CH_3O is $\nu_{as} CH_3(A') = 2904\ cm^{-1}$, being therefore red-shifted on top and bridge sites and blue-shifted on hollows (Table 2). Similar general trends have been described in the experimental study of Barros et al. [32]. On the other hand, by comparing their RAIRS data with our results for all possible sites of adsorption (Table 2), one can see that the hcp and fcc results have lower deviations than the ones from any other site. This gives further support to the conclusion reached on that experimental study, i.e., that the preferred adsorption sites for methoxy on the clean Ru surface are the hollow sites and that the tilting should be quite small (even at non-zero coverage). But, a word of caution here, remark that the CH stretch region of the RAIRS CH_3O spectra is strongly influenced by Fermi resonance between the overtones of the methyl deformations ($2 \times \delta CH_3$) and the fundamental stretching modes (νCH_3) [32,42,43], rendering difficult the assignments and forward comparisons. Lastly, Barros et al. detected also on the RAIRS spectrum a pair of νCO bands at 1045 and 1015 cm^{-1} and a $\nu_s CH_3$ band at 2822 cm^{-1}, after greatly increasing the coverage and annealing the system. The authors assigned these bands to bridging-like CH_3O species along with hollow-hcp binding. Though the present results refer to the zero-coverage limit, they point up instead to top-like species along with hollow ones.

Considering now the adsorbed CHD_2O (Table 3), one can observe that the agreement between calculations and experiments for the fundamental modes is quite good with a relative error not greater than ~2%. On the recorded RAIRS CHD_2O spectrum [46], a band at 2159 cm^{-1} has also been detected and assigned to the overtone of the symmetric bending mode ($2 \times \delta_s CD_2$). This mode is shifted up accordingly to both the calculated and experimental values for the fundamental (calc. fcc: $2 \times 1052 = 2104\ cm^{-1}$; exp.: $2 \times 1071 = 2142\ cm^{-1}$; Table 3). The up-shift and the high-intensity observed for this mode can be attributed to Fermi resonance repulsion with the fundamental $\nu_s CD_2$. Overall, this leaves no doubts on the proposed assignment of the modes and is consistent with a C_s local symmetry for the adsorbate CHD_2O (or C_{3v} for CH_3O) and a perpendicular orientation of the C–O axis. Once more, however, the present results make no distinction between the two hollow adsorption sites.

To conclude, all spectral features can be accounted for by assuming that methoxy adsorbs (or its isotopomer CHD_2O), at extremely lower coverage, in an upright orientation on either hollow sites of the clean Ru(0001) surface. The good agreement between the calculations and experiments for the IR spectra makes us confident that our chosen cluster models represent this metallic surface well.

3.1.3. Bonding analysis

To acquire further information on the electronic features of the radical–surface interaction, we have determined the density of states of methoxy adsorbed on the hollow sites of the Ru surface. As we have found similar features for both hollows, the following discussion refers only to the fcc adsorption site.

In the bottom panel of Fig. 3, the total DOS of the CH_3O_{fcc}–Ru_{18}(0001) system (solid curve) is compared to that of the clean surface (dotted curve), with the Fermi level set as the origin of the energy scale. At lower energies

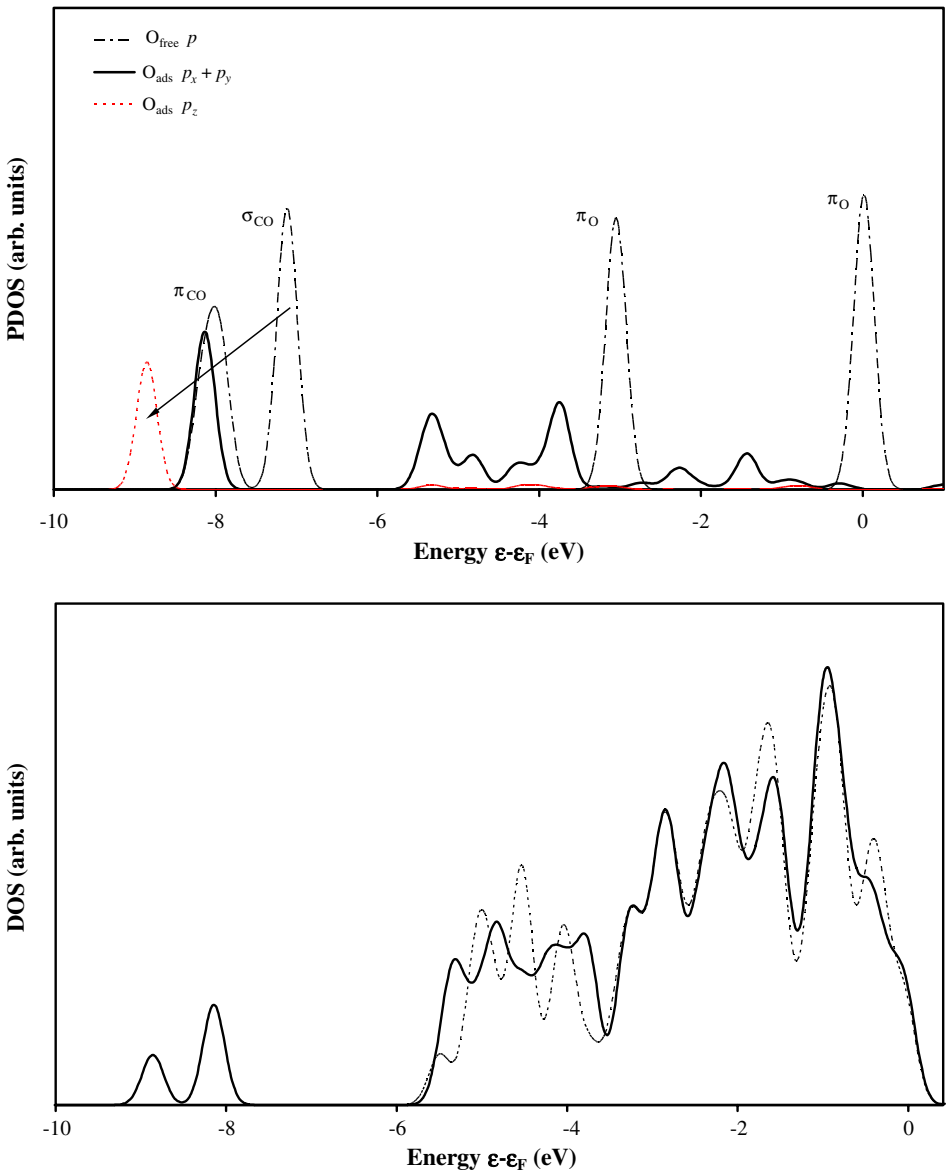

Fig. 3. Bottom panel: comparison between the DOS of the CH_3O_{fcc}–Ru(0001) system (solid curve) with that of the clean Ru surface (dotted curve). Top panel: the CH_3O projected DOS for the system CH_3O_{fcc}–Ru(0001) superimposed to the DOS of the free radical. The assignment of the energy levels on the scale is achieved by aligning the deepest level (identical for the free and adsorbed radical) from the calculations for the free and adsorbed CH_3O.

(below ~8 eV), the electron states are fully localized on the adsorbed radical and so no adsorbate-surface interaction is present, i.e., the states maintain the same character as in isolated methoxy. The band extending about 6 eV below the Fermi level is characteristic of the Ru d-orbitals. The differences between the clean and the CH_3O–Ru(0001) system, revealed by the inequivalence of the solid and dotted curves in Fig. 3, are due to the adsorbate-surface interaction. One can trace such interaction by comparing the contribution of the molecular orbitals (MO) of the adsorbed CH_3O to the total DOS of the CH_3O–Ru(0001) system with the MOs of free CH_3O (top panel of Fig. 3). In the free radical, the two higher occupied MOs correspond to non-bonding π-orbitals on the oxygen atom, being the highest one partially filled. It is clearly seen that these are the radical MOs which interact most; their bands are spread out considerably due to the mixing with the Ru d-band. The following σ_{CO} orbital is shifted down by about 2 eV, even below the degenerate π_{CO} orbitals. This leads to an σ_{CO}/π_{CO} orbital inversion, alike that observed in experiments [81] and established by DFT-periodic calculations [27] for CH_3O adsorbed on Cu(111).

3.2. Adsorption of CH_3O on the low oxygen precovered Ru(0001) surface

3.2.1. Structures and energetics

To obtain full information about the influence of co-adsorbed oxygen on the adsorption properties of the methoxy radical, first, we needed the geometric parameters related to

the adsorption of atomic oxygen on Ru(0001). These were determined by identical calculations based on the Ru_{13} cluster model (data not shown), as some tests performed with the larger clusters confirmed us that the model is adequate enough for describing the geometry of such small adsorbate. As expected [82,83], atomic oxygen is trapped strongly on the surface and do prefer the hcp hollow site of the metal surface; further, for that site, the calculated O–Ru bond length of 2.04 Å is only slightly longer than the LEED-determined value of 2.03 Å [82]. Again, the net charge of adsorbed oxygen is higher for sites where E_{ads} is greater. When compared to CH_3O (Table 1), one can see a larger discharge of the metal surface towards the adsorbate ($q_{O\,fcc} = -0.68$ e; $q_{O\,hcp} = -0.67$ e; $q_{O\,bridge} = -0.61$ e; $q_{O\,top} = -0.49$ e).

The oxygen modified Ru(0001)–(2 × 2)–O surface was modeled with the largest Ru_{28} cluster model but with three oxygen atoms placed on the hcp sites (i.e., the preferred sites for adsorbed oxygen; d(O-Surf) = 1.32 Å). Three different hollow sites labeled as fcc_1, fcc_2 and hcp can be defined on that modified surface (see Fig. 4); these were the only sites considered here. The adsorption properties of radical methoxy over those non-equivalent hollow sites are summarized in Table 4.

The bonding of CH_3O on the Ru(0001)–(2 × 2)–O surface is slightly different from that on the clean surface. Firstly, the radical is not exothermically chemisorbed at all hollow sites of the modified surface. In fact, at the fcc_1 site, the interaction is very weak and repulsive (~0.5 eV) and the radical stays at a distance too far away from the surface (2.61 Å). At the fcc_2 and hcp hollows, it is exothermically chemisorbed and also adopts an almost upright orientation, with lower interaction energy relative to the clean surface (by ~0.3 eV). The fcc2 site is the preferred position for the adsorbed radical but, again, the small energy difference between this site and the hcp site (=0.01 eV) suggests that both will be equally populated on the modified surface. The Mulliken effective charges obtained now for such sites (fcc_2: −0.22 e; hcp: −0.21 e; Table 4) may be compared to those on the clean surface (fcc: −0.25 e; hcp: −0.24 e; Table 1). They indicate a lower charge transfer from the surface to the CH_3O adsorbate, due to the co-adsorbed electronegative oxygens which deplete the surface electron density.

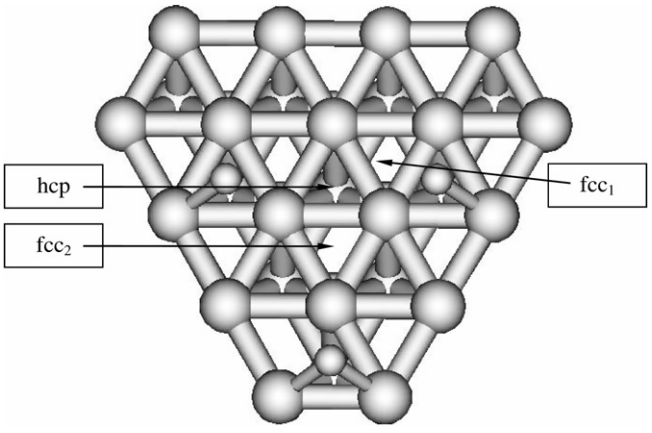

Fig. 4. Top view of the Ru_{28}(18,10) cluster used to model the adsorption of methoxy on the Ru(0001)–(2 × 2)–O surface. The position of the oxygen atoms were obtained previously by optimization on the clean surface (d(O-Surf) = 1.32 Å). The hollow adsorption sites are marked with arrows and labeled.

3.2.2. IR vibrational spectra

The calculated normal vibrational modes for CH_3O chemisorbed on the stable hollows of the oxygen modified surface are shown in Table 5. Three sets of experimental vibrations measured by RAIRS are listed as well, upon exposing firstly the surface to 0.05 L (or to 0.1 L) of CH_3OH at 90 K and then by annealing to 130 K [34]. Notice that these experiments point to an initial C_s symmetry for CH_3O at 90 K and to reorientation to a C_{3v} symmetry at 130 K. Further, only those selected modes that can be directly compared to that RAIRS data are reported in the table.

As can be seen, the calculated νCO mode is now shifted to lower wavenumbers when compared to the one corresponding to CH_3O adsorbed on the clean surface (see Table 2). This suggests a weaker C–O bond upon precoverage (note that, for instance, for methoxy on the fcc site, the CO distance is 1.43 Å on the modified surface and 1.42 Å on the clean surface.). This chemical shift induced by the co-adsorbed oxygens is also observed in the RAIRS experiments (C_{3v} result; Table 5). The effect of the O ad-atom is also apparent in the computed ρCH_3 and $\nu_{as}CH_3$ modes that are red- and blue-shifted, respectively, in agreement with experimental data. No noticeable changes are however found for the computed $\delta_s CH_3$ and $\nu_s CH_3$ modes, unlike the blue shifts observed in experiments. But that may be due to the fact that experiments do not correspond to the theoretical methoxy *isolated molecule limit* and to possible Fermi resonance couplings. On the RAIRS CH_3O spectrum at 130 K (C_{3v} local symmetry) [34], two bands

Table 4
Calculated properties of CH_3O adsorbed on the modified Ru(001)–(2 × 2)–O surface

Cluster	Site	E_{ads} (eV)	d(O-Surf) (Å)	*ang*(C–O-Surf) (°)	$q_{adsorbate}$ (a.u.)[a]
Ru_{28}(18,10)	fcc_1	+0.51	2.61	137	−0.13
	fcc_2	−2.14	1.45	178	−0.22
	hcp	−2.13	1.40	177	−0.21

[a] Effective Mulliken charges.

Table 5
Comparison of experimental and calculated vibrational wavenumbers for CH_3O adsorbed on the modified Ru(0001)–(2 × 2)–O surface

Mode[a]		Experimental			Calculated	
		90 K (C_s)[b]	90 K (C_s)[c]	130 K (C_{3v})[c]	fcc_2 (C_{3v})	hcp (C_{3v})
νCO	(A_1/A′)	1024	1015/991	991	1002	966
ρCH_3	(E/A″)	1121	1117/1092		1123	1122
ρCH_3	(E/A′)					
$\delta_s CH_3$	(E/A′)	1470			1411	1403
$\delta_{as} CH_3$	(E/A″)				1434	1439
$\delta_{as} CH_3$	(E/A′)					
$\nu_s CH_3$	(A_1/A′)	2841	2836	2837	2836	2839
$\nu_{as} CH_3$	(E/A″)	2961	2926		2917	2927
$\nu_{as} CH_3$	(E/A′)					

[a] Irreducible representations of the modes for C_{3v}/C_s symmetric species are shown in parenthesis.
[b] RAIRS data obtained upon exposure to 0.1 L of CH_3OH at 90 K [33], save for $\delta_s CH_3$ which was obtained by EELS [30].
[c] RAIRS data obtained upon exposure to 0.05 L of CH_3OH at 90 K, and then subsequent annealing to 130 K [34].

Table 6
Comparison of experimental and calculated vibrational wavenumbers for CHD_2O adsorbed on oxygen modified Ru(0001) surfaces (C_s symmetry)

Mode	Experimental		Calculated: Ru(0001)–(2 × 2)–O	
	Ru(0001)–(2 × 1)–O[a]	Ru(0001)–(2 × 2)–O[b]	fcc_2	hcp
$w CD_2 + \nu$CO	941	949	950	939
$w CD_2 + \nu$CO	1002	1013	1006	983
$\delta_s CD_2$	1078	1072	1050	1050
$\nu_s CD_2$	2116	2116	2071	2074
νCH	2950	2942	2892	2903

[a] RAIRS data obtained upon exposure of 0.01 L of CHD_2OH at 90 K [47].
[b] RAIRS data obtained upon exposure of 0.1 L of CHD_2OH at 90 K and subsequent annealing to 105 K [47].

at 2944 cm^{-1} and 2976 cm^{-1} have also been detected and assigned to the overtones $2 \times \delta_s CH_3$ and $2 \times \delta_{as} CH_3$, respectively, with borrowed intensity from the allowed $\nu_s CH_3$ mode. Those modes are shifted up by ~100 cm^{-1} judging from the calculated values for the respective fundamentals (e.g., for $2 \times \delta_s CH_3$, calc. fcc_2: 2822 cm^{-1}; hcp: 2806 cm^{-1}), though much less according to experiments (from 4–24 cm^{-1}; $2 \times \delta_s CH_3$: 2940 cm^{-1} [30] or 2920 cm^{-1} [34]).

Moving on to the adsorbed CHD_2O, Table 6 presents the calculated vibrational normal modes of this species on the hollow sites along with the RAIRS experimental data obtained upon exposing, another oxygen modified surface (the Ru(0001)–(2 × 1)–O surface), to an extremely low dose (0.01 L) of CHD_2OH at 90 K or by exposing the Ru(0001)–(2 × 2)–O surface to a higher dose (0.1 L) and subsequent annealing to 105 K; both cases point to a C_s symmetry for CHD_2O [47].

As can be seen, the calculated and experimental wavenumbers for the fundamentals agree within an error lower than 2.1% in the present surface and somewhat more in the higher oxygen covered surface (Ru(0001)–(2 × 1)–O: <4.5%). The νCH and $\nu_s CD_2$ modes are shifted to higher wavenumbers, compared to the clean surface, owing to the chemical effect of the O ad-atoms. The agreement between the calculated and experimental shifts for these fundamentals is quite good (e.g., for νCH on the Ru(0001)–(2 × 2)–O surface, exp. shift: 4 cm^{-1}; calc. fcc_2 shift: 6 cm^{-1}). In addition, on both RAIRS spectra [47], a band has been detected (at 2171 cm^{-1} for Ru(0001)–(2 × 1)–O and at 2166 cm^{-1} for Ru(0001)–(2 × 2)–O) and assigned to the overtone of the symmetric bending mode. This overtone is shifted up by 66–71 cm^{-1}, taking into account the calculated value for the fundamental $\delta_s CD_2$, but less accordingly to experiments (by 15–20 cm^{-1}) due to possibly the Fermi resonance coupling between that overtone and the fundamental stretch $\nu_s CD_2$.

Above all, the assignments are unambiguous and confirm the C_{3v} (or C_s) local symmetry for adsorbate CH_3O (or CHD_2O) on the precovered surface, at extremely low coverage, similarly to what occurs on the clean surface. Further, this adsorbate may populate both types of hollow sites – fcc_2 and hcp – of the oxygen modified Ru(0001)–(2 × 2)–O surface. The bonding geometry of methoxy seems to be not particularly affected by pre-adsorption of atomic oxygen at such low coverage.

3.2.3. Bonding analysis

Let us look first to the effects of co-adsorbed oxygen on the electronic structure of the clean surface (bottom panel of Fig. 5). The oxygen layer down shifts the Fermi level energy (by 0.27 eV) and the d-band of the metal is spread out due to the mixing with all the p-orbitals of the oxygens; in fact,

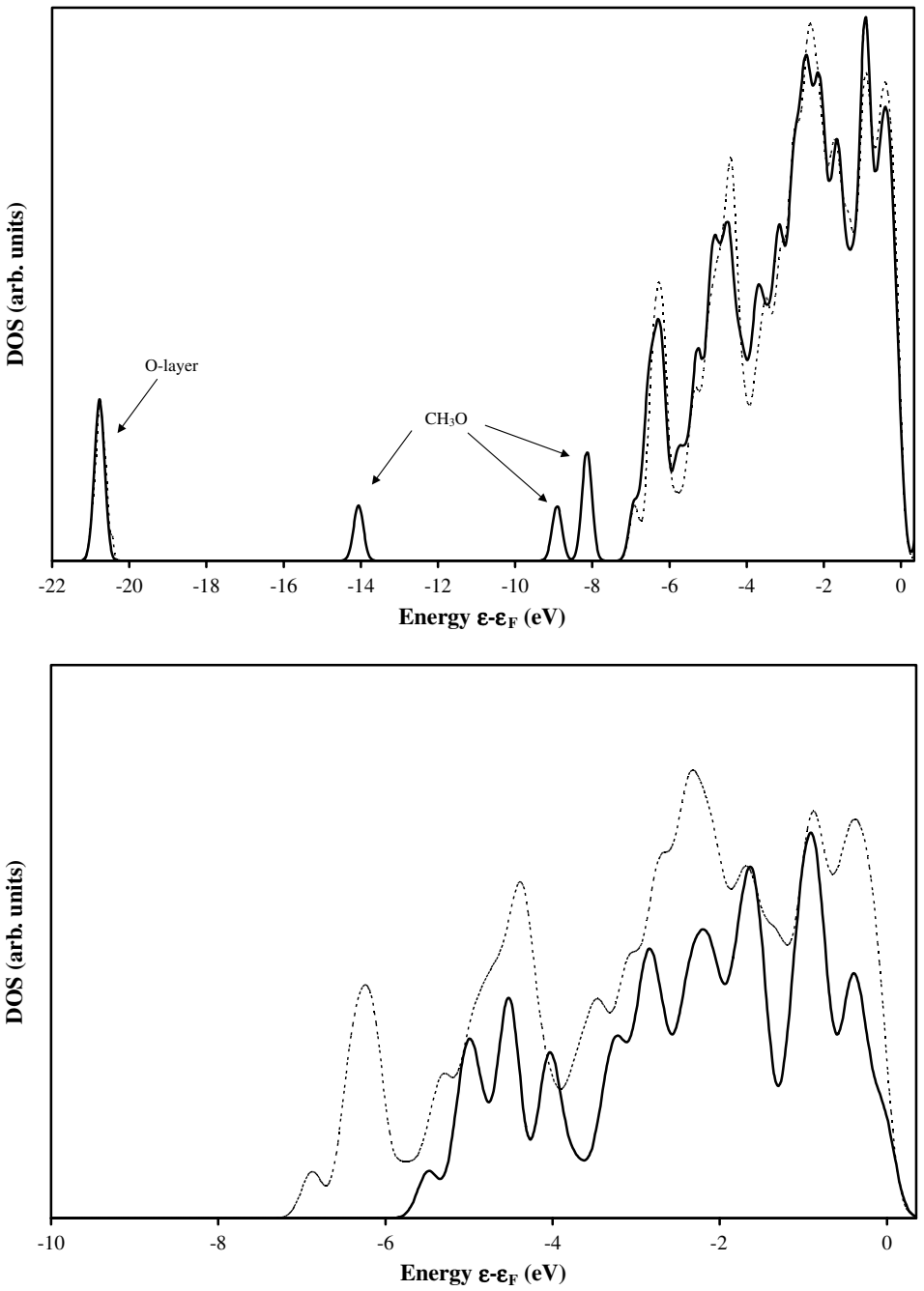

Fig. 5. Bottom panel: comparison between the DOS of the clean Ru(0001) surface (solid curve) with that of the modified Ru(0001)–(2 × 2)–O surface (dotted curve). Top panel: comparison between the DOS of the CH_3O_{fcc}–Ru(0001)–(2 × 2)–O system (solid curve) with that of the modified Ru surface (dotted curve).

by analyzing the COOP of the oxygens' p-orbitals with the Ru d-states on the modified surface, a predominantly bonding O–Ru interaction is seen as the main antibonding resonance lies above the Fermi level. In addition, the d-band center (center of the local partial DOS with respect to the Fermi level) is shifted down by 0.6 eV, which suggests a weaker bonding of the methoxy adsorbate on the basis of the d-band center model [84]. This correlates well with the finding that the computed binding energies are smaller on the Ru(0001)–(2 × 2)–O surface than on clean Ru(0001). On the other hand, new bands appear now on the lower energy region (<−20 eV; data not shown) that correspond to the core energy levels of the oxygen atoms.

In the top panel of Fig. 5, the total DOS for the most preferred adsorption site of CH_3O on the oxygen modified surface (hollow fcc) is shown and compared to the DOS of the Ru(0001)–(2 × 2)–O system, by setting the Fermi level set as the origin of the energy scale. At lower energies, the electron states are fully localized either on the adsorbed radical, similarly to the clean Ru surface, or on the O-layer

and the most important changes occur in the range of 7 eV below the Fermi level. It can be also seen that the low-energy core levels of the adsorbed CH_3O and those of the oxygen atomic layer are well separated.

Further details concerning the radical–surface interaction can be attained by determining the COOPs. As Fig. 6 shows, the shape of the COOP for CH_3O–Ru on the Ru(0001)–(2×2)–O surface does not change much with respect to the analogous COOP of the clean surface. Most importantly, the anti-bonding states are slightly pushed below the Fermi level, thereby indicating a weaker adsorbate–surface interaction on the modified surface.

Let us now look on how the bonds change upon adsorption at the oxygen modified surface (Fig. 7). On going from Ru(0001) to Ru(0001)–(2×2)–O, the net CO overlap population (OP) decreases, while that of the CH bonds is roughly the same (Ru(0001): $OP_{CO} = 0.010$, $OP_{CH} = 0.181$; Ru(0001)–(2×2)–O: $OP_{CO} = 0.005$, $OP_{CH} = 0.179$). Consequently the CO bonds are predicted to be weakened on the precovered surface. The next step is to analyze possible intermolecular interactions. By doing so, one can see that there is no O–O interaction from the preadsorbed oxygen atoms, and also the methoxy H's and the O's of the oxygen atomic layer do not develop any bonding interaction. Thus, from a bonding perspective, the important change for CH_3O adsorption on the low precovered surface relative to the clean one is a weaker CH_3O–Ru interaction. Further, the adsorbed radical is expected to dissociate or desorb more easily on the modified surface but with no participation from the co-adsorbed oxygen atoms.

4. Conclusions

The interaction of methoxy with the clean and oxygen modified Ru(0001) surfaces was investigated using a cluster model approach and DFT calculations. The results reported here show that cluster models of ca. 20–30 atoms give a reasonable description of such surfaces allowing a good prediction of the structural and energetic features of the methoxy adsorbate.

Radical methoxy is found to remain specifically adsorbed in all possible sites of the clean surface. Nonetheless, the hollow sites are favored and CH_3O- adopts a C_{3v} conformation with the C–O bond perpendicular to the surface. The computed vibrational frequencies for those hollow sites are in good agreement with the experimental RAIRS data. The adsorbate-surface interaction leads to a σ_{CO}/π_{CO} orbital inversion, similar to that already observed for Cu(111) [81] and confirmed by DFT-periodic calculations [27]. The adsorption of methoxy at either hollow site produces an estimated net charge transfer of ~0.3 e from the metal to the radical. Co-adsorbed oxygen reduces the charge transfer and has a destabilization effect on the adsorption of methoxy on the Ru(0001) surface. This correlates with the finding that the valence d-band center is lower on the oxygen precovered surface than on Ru(0001). But the bonding geometry of methoxy is not particularly affected by pre-adsorption of atomic oxygen at such low coverage. Moreover, the adsorbed radical is expected to dissociate or desorb more easily on the modified surface but with no participation from the oxygen adatoms, confirming the experimental findings.

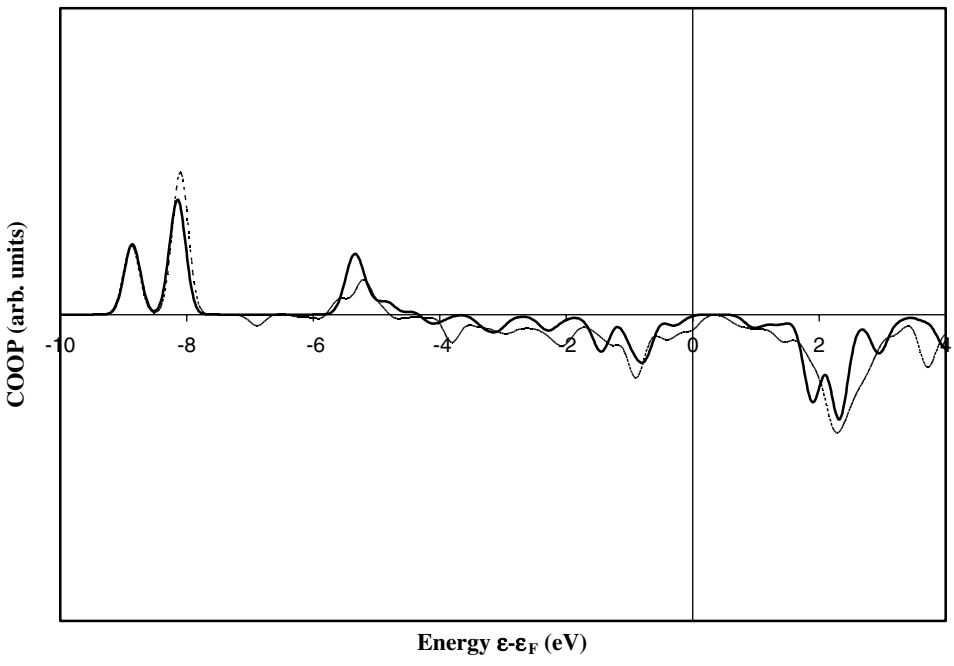

Fig. 6. COOP for CH_3O adsorbed on the fcc site over the clean Ru(0001) surface (solid curve) and over the Ru(0001)–(2×2)–O surface (dotted curve).

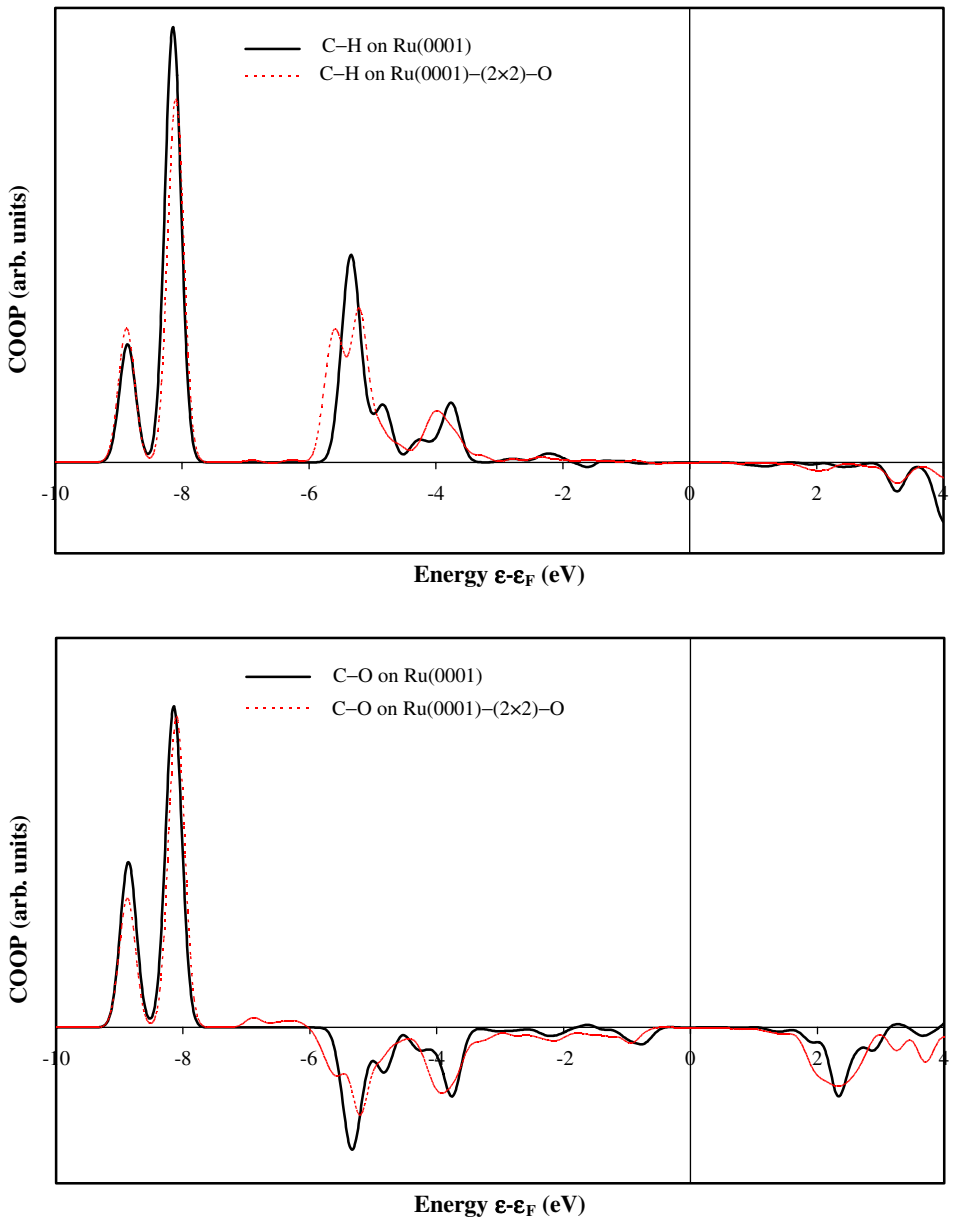

Fig. 7. Bottom panel: COOP for the methoxy C–O bond on Ru(0001) and on Ru(0001)–(2 × 2)–O. Top panel: COOP for the methoxy C–H bonds on Ru(0001) and on Ru(0001)–(2 × 2)–O.

Acknowledgement

This work was supported by Fundação para a Ciência e a Tecnologia (F.C.T.), Project POCTI/33765/QUI/2000.

References

[1] J.M. Thomas, W.J. Thomas, Principles, Practice of Heterogeneous Catalysis, VCH Publications Weinheim, Germany, 1997.
[2] H. Yoon, M.R. Stouffer, P.J. Dubt, F.P. Burke, G.P. Curran, Energy Prog. 5 (1985) 78.
[3] J.M. Tatibouet, Appl. Catal. A 148 (1997) 213.
[4] E. Reddington, A. Sapienza, B. Gurau, R. Viswanathan, S. Sarangapani, E.S. Smotkin, E.T. Mallouk, Science 280 (1998) 1735.
[5] B. Peppley, J. Amphlett, L. Kearns, R. Mann, Appl. Catal. A 179 (1999) 21.
[6] J. Greeley, M. Mavrikakis, J. Am. Chem. Soc. 124 (2002) 7193.
[7] F. Boccuzzi, A. Chiorino, A. Manzoli, J. Power Sources 118 (2003) 304.
[8] W.D. King, J.D. Corn, O.J. Murphy, D.L. Boxall, E.A. Kenik, K.C. Kwiatkowski, S.R. Stock, C.M. Lukehart, J. Phys. Chem. B 107 (2003) 5467.
[9] M.K. Weldon, C.M. Friend, Chem. Rev. 96 (1996) 1391.
[10] M. Mavrikakis, M.A. Barteau, J. Mol. Catal. A: Chem. 131 (1998) 135.
[11] W.T. Lee, F. Thomas, R.I. Masel, Surf. Sci. 418 (1998) 479.
[12] L. Diekhoner, D.A. Butler, A. Baurichter, A.C. Luntz, Surf. Sci. 409 (1998) 384.
[13] M. Endo, T. Matsumato, J. Kubota, K. Domen, C. Hirose, J. Phys. Chem. B 104 (2000) 4916.
[14] V. Efstathiou, D.P. Woodruff, Surf. Sci. 526 (2003) 19.
[15] G.-C. Wang, Y.-H-. Zhou, J. Nakamura, J. Chem. Phys. 122 (2005) 044707.

[16] M. Witko, K. Hermann, J. Chem. Phys. 101 (1994) 10173.
[17] J.R.B. Gomes, J.A.N.F. Gomes, F. Illas, Surf. Sci. 443 (1999) 165.
[18] J.R.B. Gomes, J.A.N.F. Gomes, J. Mol. Struct. (Theochem) 503 (2000) 189.
[19] J.R.B. Gomes, J.A.N.F. Gomes, Surf. Sci. 471 (2001) 59.
[20] J.D. Head, Y. Shi, Int. J. Quant. Chem. 75 (1999) 815.
[21] J.D. Head, Int. J. Quant. Chem. 77 (2000) 350.
[22] Y. Ishikawa, M.-S. Liao, C.R. Cabrera, Surf. Sci. 463 (2000) 66.
[23] K. Nakatsuji, Z.-M. Hu, Int, J. Quant. Chem. 77 (2000) 341.
[24] J. Greeley, M. Mavrikakis, J. Catal. 208 (2002) 291.
[25] M.P. Andersson, J. Blomquist, P. Uvdal, A.D. MacKerell, J. Phys. Chem. B 106 (2002) 7193.
[26] Z.-X. Chen, K.M. Neyman, K.H. Lim, N. Rosch, Langmuir 20 (2004) 8068.
[27] S. Sakong, A. Grob, J. Catal. 231 (2005) 420.
[28] W.S. Sim, P. Gardner, D.A. King, J. Phys. Chem. 99 (1995) 16002.
[29] J. Hrbek, R.A. dePaola, F.M. Hoffman, J. Chem. Phys. 81 (1984) 2818.
[30] J. Hrbek, R. dePaola, F.M. Hoffman, Surf. Sci. 166 (1986) 361.
[31] T. Sasaki, Y. Itai, Y. Iwasawa, Surf. Sci. 443 (1999) 44.
[32] R.B. de Barros, A. RGarcia, L.M. Ilharco, J. Phys. Chem. B 105 (2001) 11186.
[33] R.B. de Barros, A.R. Garcia, L.M. Ilharco, Surf. Sci. 502–503 (2002) 156.
[34] R.B. de Barros, A.R. Garcia, L.M. Ilharco, J. Phys. Chem. B. 108 (2004) 4831.
[35] L.J. Richter, W.J. Ho, J. Chem. Phys. 83 (1985) 2569.
[36] J.S. Huberty, R.J. Madix, Surf. Sci. 360 (1996) 144.
[37] M.K. Weldon, P. Uvdal, C.M. Friend, J.G. Serafin, J. Chem. Phys. 103 (1995) 5075.
[38] S.M. Johnston, A. Mulligan, V. Dhanak, M. Kadodwala, Surf. Sci. 530 (2003) 111.
[39] J.P. Camplin, E.M. McCash, Surf. Sci. 360 (1996) 229.
[40] M.A. Chester, E.M. McCash, Spectrochim. Acta A 43 (1987) 1625.
[41] K. Mudalige, S. Warren, M. Trenary, J. Phys. Chem. B 104 (2000) 2448.
[42] R. Ásmundsson, P. Uvdal, J. Chem. Phys. 112 (2000) 366.
[43] M.P. Andersson, P. Uvdal, A.D. McKerrel Jr., J. Phys. Chem. B 106 (2002) 5200.
[44] M.P. Andersson, P. Uvdal, Surf. Sci. 549 (2004) 87.
[45] M.P. Andersson, J. Blomquist, P. Uvdal, J. Chem. Phys. 123 (2005) 224714.
[46] R.B. de Barros, A.R. Garcia, L.M. Ilharco, Surf. Sci. 572 (2004) 277.
[47] R.B. de Barros, A.R. Garcia, L.M. Ilharco, Chem. Phys. Chem. 6 (2005) 1299.
[48] R.B. de Barros, A.R. Garcia, L.M. Ilharco, Surf. Sci. 600 (2006) 2425.
[49] A.S.S. Pinto, R.B. de Barros, M.N.D.S. Cordeiro, J.A.N.F. Gomes, A.R. Garcia, L.M. Ilharco, Surf. Sci. 566–568 (2004) 965.
[50] M. Melle-Franco, G. Pacchioni, A.V. Chadwick, Surf. Sci. 478 (2001) 25.
[51] A. Valcarcel, J.M. Ricart, A. Clotet, A. Markovits, C. Minot, F. Illas, J. Chem. Phys. 116 (2002) 1165.
[52] J.R.B. Gomes, F. Illas, N. Cruz Hernández, J.F. Sanz, A. Wander, N.M. Harrison, J. Chem. Phys. 116 (2002) 1684.
[53] D. Domínguez-Ariza, C. Sousa, N.M. Harrison, M.V. Ganduglia-Pirovano, F. Illas, Surf. Sci. 522 (2003) 185.
[54] A. Gil, A. Clotet, J.M. Ricart, G. Kresse, M. García-Hernández, N. Rosch, P. Sautet, Surf. Sci. 530 (2003) 71.
[55] G.-C. Wang, L. Jiang, Y. Morikawa, J. Nakamura, Z.-S. Cai, Y.-M. Pan, X.-Z. Zhao, Surf. Sci. 570 (2004) 205.
[56] C.S. Tautermann, D.C. Clary, Phys. Chem. Chem. Phys. 8 (2006) 1437, and references therein.
[57] D.R. Lide (Ed.), CRC Handbook of Chemistry and Physics, CRC Press, Boca Raton, FL, 1997.
[58] A.D. Becke, J. Chem. Phys. 98 (1993) 5648.
[59] M.J. Frisch, G.W. Trucks, H.B. Schlegel, G.E. Scuseria, M.A. Robb, J.R. Cheeseman, V.G. Zakrzewski, J.J.A. Montgomery, R.E. Stratmann, J.C. Burant, S. Dapprich, J.M. Millam, A.D. Daniels, K.N. Kudin, M.C. Strain, O. Farkas, J. Tomasi, V. Barone, M. Cossi, R. Cammi, B. Mennucci, C. Pomelli, C. Adamo, S. Clifford, J. Ochterski, G.A. Petersson, P.Y. Ayala, Q. Cui, K. Morokuma, N. Rega, P. Salvador, J.J. Dannenberg, D.K. Malick, A.D. Rabuck, K. Raghavachari, J.B. Foresman, J. Cioslowski, J.V. Ortiz, A.G. Baboul, B.B. Stefanov, G. Liu, A. Liashenko, P. Piskorz, I. Komaromi, R. Gomperts, R.L. Martin, D.J. Fox, T. Keith, M.A. Al-Laham, C.Y. Peng, A. Nanayakkara, M. Challacombe, P.M.W. Gill, B. Johnson, W. Chen, M.W. Wong, J.L. Andres, C. Gonzalez, M. Head-Gordon, E.S. Replogle, J.A. Pople, Gaussian Inc., Pittsburgh PA, 2001.
[60] S.H. Vosko, L. Wilk, M. Nusair, Can. J. Phys. 58 (1980) 1200.
[61] C. Lee, W. Yang, R.G. Parr, Phys. Rev. B 37 (1988) 785.
[62] A. Ricca, C.W. Bauschlicher, J. Phys. Chem. 98 (1994) 12899.
[63] T.V. Russo, R.L. Martin, P.J. Hay, J. Chem. Phys. 102 (1995) 8023.
[64] P.E.M. Siegbahn, R.H. Crabtee, J. Am. Chem. Soc. 119 (1997) 3103.
[65] T. Jacob, W.A. Goddard, J. Phys. Chem. 109 (2005) 297.
[66] P.J. Hay, W.R. Wadt, J. Chem. Phys. 82 (1985) 270.
[67] P.J. Hay, W.R. Wadt, J. Chem. Phys. 82 (1985) 284.
[68] P.J. Hay, W.R. Wadt, J. Chem. Phys. 82 (1985) 299.
[69] R.P. Messmer, S.K. Knudson, K.H. Johnson, J.B. Diamond, C.Y. Yang, Phys. Rev. B 13 (1976) 1396.
[70] R. Hoffmann, Solids and Surfaces: A Chemists View of Bonding in Extended Structures, VCH, New York, 1988.
[71] N.M. O'Boyle, GaussSum 2.0, 2006. Available at <http://gausssum.sf.net>.
[72] D. Menzel, Surf. Rev. Lett. 6 (1999) 835, and references therein.
[73] J.D. Head, Int. J. Quant. Chem. 65 (1997) 827.
[74] A.P. Scott, L. Radom, J. Phys. Chem. 100 (1996) 16502.
[75] S.F. Boys, F. Bernardi, Mol. Phys. 19 (1970) 553.
[76] J.M. Ricart, J. Rubio, F. Illas, P.S. Bagus, Surf. Sci. 304 (1994) 335.
[77] K.M. Neyman, C. Inntam, A.B. Gordienko, I.V. Yudanov, N. Rösch, J. Phys. Chem. B 108 (2004) 5424.
[78] F. Martin, H. Zipse, J. Comput. Chem. 26 (2005) 97, and references therein.
[79] A.E. Reed, L.A. Curtiss, F. Weinhold, Chem. Rev. 88 (1988) 899.
[80] C.J. Nelin, P.B. Bagus, M.P. Philpott, J. Chem. Phys. 87 (1987) 2170.
[81] D.E. Ricken, A.W. Somers, J. Robinson, A.M. Bradshaw, Faraday Disc. Chem. Soc. 89 (1990) 291.
[82] M. Lindroos, H. Pfnür, G. Held, D. Menzel, Surf. Sci. 222 (1989) 451.
[83] C.-T. Au, C.-F. Ng, M.-S. Liao, J. Catal. 185 (1999) 12.
[84] M. Mavrikakis, B. Hammer, J.K. Norskov, Phys. Rev. Lett. 81 (1998) 2819.